[1]Gireesh T. K.

[2] Senthilkumar S.

Designing a Novel Learning Approach for Infectious Lung Disease Prediction using Bi-Directional Recurrent Neural Network (BRNN)

JES Journal of Electrical Systems

Abstract: - The principal goal of this research is to use regular imaging to diagnose and classify several lung disorders, including pneumonia, COVID-19 and tuberculosis.A novel Bi-directional Recurrent Neural Network (BRNN) model is implemented in this work to categorize the disease according to the input samples given. With the help of the feature extractor, prediction model, and classification model, the suggested model performs feature analysis. The E2E model that has been suggested carries out knowledge acquisition using an efficient computational and memory approach. The benchmark dataset, made accessible online, was used to test the proposed model. When networks are trained to extract characteristics, the developments in deep learning techniques yield encouraging results and offer higher potential efficiency than biomedical applications. The main goal is to evaluate the significance of current methods and validate the BRNN model to address the concerns that are currently present. The suggested model offers better efficiency and performance for better detection. The results reveal that the model with a recurrent network works better than the current methods, with an accuracy of 71% for all diseases, whereas the traditional network models perform worse. The suggested model has less computational overhead and fewer training parameters. When compared to alternative methods, the model offers a superior trade-off.

Keywords: Deep learning, Prediction, Tuberculosis, Pneumonia, COVID-19

1. Introduction

Several reasons have contributed to the rise in the mortality rate from lung diseases over the last few years. Among the mild to moderate adverse effects that those infected with new COVID-19 and pneumonia may suffer include fever, hacking, and dyspnea [1]. On the other hand, severe pneumonic illnesses in the lungs have claimed the lives of several persons. High chest obstruction (pneumonia) caused a fast drop in oxygen levels and catastrophic cardiovascular failure in a significant number of deaths associated with the coronavirus [2]. In contrast, the little air sacs in the human lungs become inflamed when a lung illness called pneumonia strikes. It could be challenging to unwind because it removes a lot of liquid. Pneumonia can be brought on by various conditions, including colds, bacterial infections, and viral infections (such as COVID-19, bacterial influenza, or viral pipe) [3]. Distinguishing between Covid-10 pneumonia and widespread/bacterial pneumonia from chest X-ray pictures is a very moving task for clinical professionals due to the emergence of COVID-19 illness [4]. Thus, this paper focuses on the early identification and categorization of infectious lung diseases based on unrefined X-ray pictures to provide appropriate therapy and reduce the mortality rate associated with high chest blockages. Novel Coronavirus Infected Pneumonia (NCIP) is the name given to lung illness caused by a novel COVID-19 [5].

Chest imaging methods, including X-rays and CT, are frequently used to identify various lung diseases. Radiologists and physicians utilize CT and X-ray images to diagnose lung diseases. When comparing the results of the X-ray and CT sweep, the X-ray method is more practical and produces comparable results [8]. As a result, several experts recommended chest X-rays to check for lung infections, especially in the Covid-19 era.Medical practitioners have been examining and analyzing the various abnormalities in the human body's organs such as the teeth, bones, head, chest, and so forth—for a very long time using X-ray technology. Numerous studies have found that X-rays are a valuable method for diagnosing illnesses while revealing compulsive changes and their cost-effectiveness and non-intrusive qualities [9]. Chest X-ray pictures can be used to diagnose lung disorders shown as solidifications, dimmed costophrenic points, widely dispersed knobs, cavitations, and invades. Radiologists identify a few problems while examining the patient's X-ray image: pericarditis, pneumonia, nodules, pleurisy, radiation, invasion, fractures, and pneumothorax.

Scientists carefully thought about programming lung infection detection, as they believe that radiologists find and organize lung illnesses using X-ray pictures of the chest to be a complex interaction. For the past ten years, several Computer-Aided Diagnosis (CAD) frameworks have been developed using X-ray images [10]. However, these frameworks needed to provide the information required for pulmonary disease diagnosis and orders. Since it is critical to identify the relationship between lung pneumonia and its affiliation with bacterial or viral contaminations, the innovative COVID-19 assisted lung illnesses even more, making the duties for such

[1]Research Scholar, Dept of Computer Science & Engineering, Vinayaka Mission's Kirupananda Varier Engineering College, Vinayaka Mission's Research Foundation (DU)
Salem, Tamil Nadu, India gireeshtk@gmail.com
[2]Associate Professor, Dept of Computer Science & Engineering. Vinayaka Mission's Kirupananda Varier Engineering College, Vinayaka Mission's Research Foundation (DU)
Salem, Tamil Nadu, India vmkvec.itsenthilkumar@gmail.com

CAD frameworks more challenging [11].It is easier to focus on pneumonic patients with this configuration. Many efforts have been made since the COVID-19 incident to provide a computer-aided detection (CAD) framework for localizing coronavirus and pneumonia infections using pictures from chest X-rays, deep learning techniques, and robotized image handling. Deep learning requires a more involved process for preparing and identifying the entire dataset because it is an automated element learning and extraction technique [12]. Consequently, these systems could be more robust and resilient to the growing datasets. Because of its ability to increase precision and perform programmed feature extraction, deep learning techniques like Convolutional Neural Networks (CNN) have gained significant attention in diagnosing lung diseases [13]. However, these techniques must be improved due to the critical processing time and space needs that develop when input photos automatically learn features. Furthermore, deep learning-based systems face challenges, including more excellent miss classification rates and disappearing gradient explosion [14]. Most of these systems rely on automatically generated features from 3D input images containing considerable oscillations. Another explanation for the increased space and time requirements is that the present methods assign the CNNs the responsibility of feature extraction and categorization [15].

1.1. Research Motivation

It looked at approaches primarily using deep learning CNN models for automatic feature extraction. Using the pre-trained models, the majority of the strategies used the transfer learning process [16]. The primary objective of each of the previously stated systems was the automated categorization of pulmonary diseases from chest MRI pictures. Despite the encouraging results of such CAD systems, there are still considerable challenges in classifying lung disorders using chest X-ray pictures. These difficulties are summed up Improving image quality is different from the objective of any state-of-the-art technique [17]. The inability of the CNN models to generate the necessary ROI-specific features from the low-quality X-ray pictures restricts the validity of the suggested models. 2D input was considered when designing the 2D-CNN models to extract features requiring more processing power and memory. A computationally inefficient CAD system is produced when lung illnesses are automatically classified using a 2D network model [18]. The CNN models create the high-dimensional features vector, which comprises notable differences between each extracted feature. Such variations result in the worst error surface shape, lengthy training and optimization stuck in a local optimal state. The performance of classification is also impacted. They only implemented the scaling feature but encountered further issues [19]. The minimum test sample size and maximum training sample size employed in the performance analysis of cutting-edge research place limits on the scalability of CAD systems.

In light of the preceding justifications and observations, to achieve accurate lower limb movement categorization, they offer a transfer-learning-based deep learning system called a single, unified platform in this paper, which predicts lung disease from four different datasets [20]. The Bi-directional Recurrent Neural Network (BRNN)is used in constructing the suggested framework to take advantage of the data-driven feature engineering property and eliminate the need for time-consuming manual feature extraction and selection processes. Because the BRNN is hierarchical, it also provides data-driven end-to-end learning from the raw data [21]. High-level feature extraction is made possible, helping to understand, distinguish, and separate the clinical patterns from the hidden information in the data. Thus, it enhances performance by eliminating the requirement for subject expertise. Furthermore,a computationally effective memory architecture is created [22]. This is accomplished by feeding the classification model with the knowledge from a model trained to predict lung disease due to COVID-19 and tuberculosis. This work is novel in developing a hybrid deep-learning model that is accurate and capable of predicting COVID-19 and tuberculosis information from the provided dataset [23]. In circumstances where physiotherapists and other skilled doctors are absent, this paradigm is fundamental for remotely monitoring rehabilitation progress. The suggested model was effectively tested using publicly accessible datasets for lung disease prediction, which includes various subjects. We could classify lung disease among participants with affected and healthy subjects with average accuracy. Researchers also observed that the mean absolute inaccuracy [24]. The Bi-directional Recurrent Neural Network (BRNN)model's efficacy in assessing rehabilitation conditions is demonstrated by the classification of lung disease and the precise prediction of COVID-19 and tuberculosis [25]. This is particularly true for patients with pathologies, for whom sample data is essential to determining the general state of affairs in remote monitoring scenarios.

2. Related works

This section discusses various existing approaches used for predicting lung based diseases. CNNs are one of the most excellent methods available today for medical image analysis, as they are incredibly effective at classifying images.A handful of the most modern CNN models covered in the following sections are Sequential, Functional, and Pre-Trained. Three distinct use cases for CNN-trained models in tuberculosis detection were proposed by Liu et al. The second suggestion uses conference resolution (CR) to extract features, which are then trained in SVM classifiers. In contrast, the other three ways features are derived from CNN architectures and trained in SVMs [26]. These two ideas are merged to form an ensemble of the classifiers in the third suggestion. The Shenzhen dataset comprises sixty-six X-ray images, whereas the Montgomery dataset contains 138

radiographs. These honed models aid in speeding up processing, but their poor accuracy makes them unsuitable for use in diagnosing medical conditions. The mask RCNN technique was proposed with the ability to extract both local and global characteristics; the model is a deep neural network [27]. The division of pixels is done, and this approach is anticipated to perform better when tested on the radiograph dataset.

This method makes the affected areas stand out and offers a heat map so that those examining the data can make sense of it more easily. However, they have ensembled the Mask RCNN models ResNet50 and ResNet101, which, when trained, require more GPU processing power and offer less biased outcomes than expected [28]. The authors used four distinct models for their presentations. ResNet152v2 and MobileNetV2 are the specific models that were employed. The two models utilized from the start were CNN and LSTM-CNN out of the four. A deep learning neural network model was created from the ground up to recognize the signs of pneumonia from chest X-ray images. Among its many drawbacks is its enormous design; it has hundreds of millions of weights for trainable parameters [29]. High processing and computational power are needed for this kind of model. Using various deep learning methods, the author created a model for classifying and identifying lung nodules on computed tomography (CT) images. To prevent a delay in diagnosis, the CT scans needed to use the maximum level of accuracy and a computer-aided detection technique to distinguish between benign and malignant lung nodules. The classification of lung nodules is enhanced when comparing the outcomes of deep learning techniques to alternative approaches.The accuracy of the classification system quickly rose once the mutations were incorporated into the deep learning architecture. The new effects in nodule classification were identified, and the early stages of a malignant lesion were determined using the deep learning approach [30].

Decompose, Transfer, and Compose (DeTraC) was the deep learning model created to mimic the characterization of COVID-19 disease using X-ray pictures. The DeTraC approach performed well when managing abnormalities in information. CNNs were again designed for the pneumonia grouping, utilizing the X-ray and CT filter images and the VGG-19 transformation, decision tree, and Inception V2 [30]. A method for automatically recognizing and classifying COVID-19 illnesses was proposed. By assembling a dataset from participants in traditional and COVID-19 studies, they do so by gathering chest X-ray scans. To anticipate planned infections, they created and evaluated a CNN model. The COVIDDetectioNet master-planned model was introduced to characterize COVID-19 from chest X-ray images. They utilized resources from multiple deep components. They combined a transfer learning approach with a pre-built CNN-assisted AlexNet model. They support the determination approach to identify the most effective elements from each deep learning design layer. At that point, grouping was done using SVM's delicate registering approach.The identification and categorization of COVID-19 disease into three groups—viral pneumonia, bacterial pneumonia, and the usual class was made possible using a technique reported [30]. They used a deep transfer learning technique to apply the theory to several chest X-ray datasets of various sizes. A pair of ensemble deep transfer learning frameworks were created to identify COVID-19 infections from a chest X-ray image.They enhanced recognition performance by using the pre-prepared models. They posed as viral, bacterial, and coronavirus pneumonia. Table 1 depicts the comparison of various prevailing approaches.

Table 1 Comparison of various prevailing approaches

References	Applications	Methods	Merits	Demerits
[18]	Predict pre-invasive, benign and invasive lung nodes	CT with machine learning approaches	Improved accuracy and earlier detection	Larger training data and risk for false positive values
[19]	Lung disease screening	Lesser dose CT and CT image datasets using deep learning approaches	Enhanced access with constraint resources	Lesser sample size
[20]	Prediction and identification of pulmonary nodules	Deep learning and CT lung datasets	Enhanced accuracy and efficiency	Lesser sample size
[22]	CT images for predicting lung diseases	Enhanced clustering and deep learning with trained neural networks and CT scans	Accuracy with traditional clustering-based approach with lesser training time	It needs enormous parameters and higher training time compared to various other approaches.
	Histopathological images with CT image scans	Various deep learning approaches like CNN, VGG-19, VGG-16, ResNet	Ability to learn training data with effectual cost function within gradient descent where constant assessment	Integration needs to be improved with fuzzy genetic optimization approaches that have

[24]		50 and Inception V3	towards accuracy and updated parameters	enhanced efficiency and performance.
[26]	Improved cell prediction with hybrid neural networks to haul out features from CT scans using learning approaches	3DCNN with RNN for disease classification in lung nodes and adopts LUNA 16 dataset	Classification with superior sensitivity, accuracy, selectivity and so on	Improved efficiency by data integrity, which is not adopted in the proposed approach
[27]	Diverse convolutional layers to execute detection from CT scan imaging	A CNN-based model with higher accuracy for earlier lung disease with CT scan images.	CNN with higher accuracy and earlier lung disease prediction and diminishes false positives	Constrained epochs and training samples

3. Methodology

The datasets that were used, the pre-processing, the methods for augmenting the data, and the various algorithms employed are all covered in this section. Fig 1 shows a flowchart representation of the suggested technique's workflow.

3.1. Network model

The suggested network architecture of the Bi-directional Recurrent Neural Network (BRNN) model is shown in Fig 1. It consists of blocks for movement categorization, prediction, and feature extraction. Consequently, the first stage comprises four convolutional layers that use the Relu activation function to work in parallel. Max-pooling and dropout layers come next to assemble every feature from every channel simultaneously. In this study, all the samples were considered for the input. Before entering the second stage, all of the obtained feature maps are concatenated. The dropout layer and max pooling are layered after the single convolutional layer with the ReLU activation function that makes up the second stage. The classification block and the predictor block then simultaneously receive the output of the feature extractor block for processing. The RNN predictor block predicts the features using two layers of LSTM units with linear activation functions and a dense layer, using information taken from the input data. Likewise, the classification block is made up of the softmax loss function, dense layer, and flattened layer, which aids in the classification of motions according to the features that were retrieved.

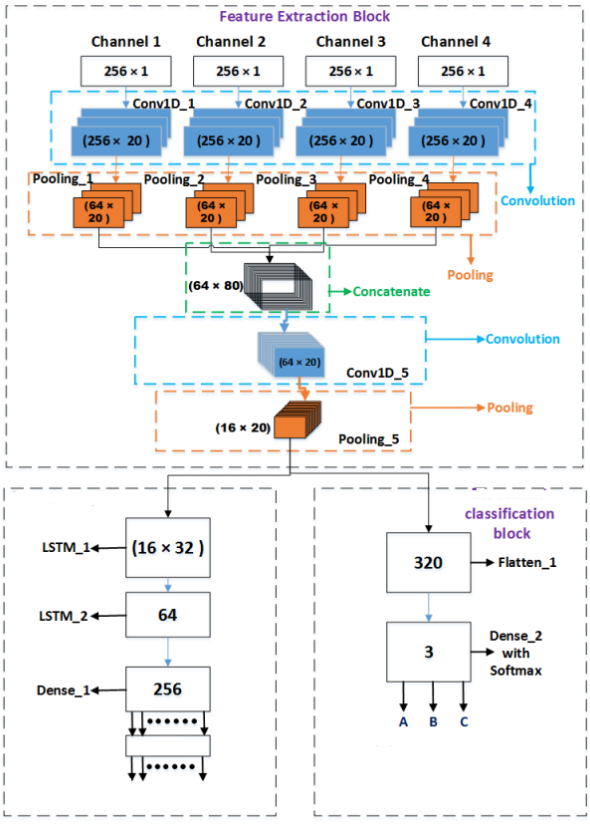

Fig 1 Architecture diagram

The optimally tuned hyper-parameters primarily influence the RNN model's performance. These parameters fall into two categories: training parameters and architectural parameters. The architectural parameters were selected by considering the number of filters or kernels in each layer, the number of layers overall, the size of each filter, the stride rate, and the pooling size. However, as training parameters, it uses many variables, including the number of epochs, activation function, loss function, dropout rate, learning rate, and back-propagation technique. Within each convolutional in the feature extractor block, each of the 20 filters in the suggested model has a max-pooling size of 4 × 1 and a size of 11 × 1. 16640 neurons were coupled to 256 outputs in the dense layer of the predictor block which included the first and second LSTM layers, each having 32 or 64 memory units in size. For the movement categorization block in the dense layer, 963 neurons with three outputs each were employed. To train the model, the following parameters were set: batch size of 25, 70 epochs, Adam optimizer with a default learning rate of 0.001, and dropout with a 50% probability threshold. These architectural specifications for BRNN are listed in Table 1. Heuristic grid search to optimize the obtained hyper-parameters produced better results than state-of-the-art techniques.COLAB was set up as the backend engine for the simulation environment where BRNN underwent training and evaluation. The hardware consisted of a Lenovo ThinkStation with 32 GB of RAM and an Intel Xeon CPU E5-2650 v2 processor operating at 2.6 GHz, running 64-bit Windows OS. After training the model to predict features, the transfer learning methodology was used to classify illness using the pre-existing features and feature extractor block settings. A more affordable way to handle the inference phase is to allow the feature extractor block's weights and parameters to be shared for both classification and prediction. Algorithm 1 depicts the model functionality.

Algorithm 1:

1. Initialize input dataset D; //COVID19 and Tuberculosis dataset
2. For all $i = 1, \dots, n$ where n is no. of iterations
3. Predict the local maxima $p^i(n)$ and local minima as $q^i(n)$
4. Predict the consecutive maxima for all values;
5. Evaluate the weight and bias values of the proposed network model;
6. Initialize Conv1D_1 to Conv1_4 and pooling_1 and pooling_4 with weight and bias;
7. Initialize stage 2 layers;
8. Initialize Conv1D_5 and Pooling_5 with weight and bias;
9. Initialize the prediction and classification module with Conv1D and pooling layer outputs;
10. Execute flatten layer; //
11. Determine the classification outcomes with class labels;

Table 2 Parameter description

Block			Network model	
			Output	Bias and weights
Feature extraction	Stage 1	Input_1	256, 1	0
		Input_2	256, 1	0
		Input_3	256, 1	0
		Input_4	256, 1	0
		Conv1D_1	256, 20	240
		Conv1D_2	256, 20	240
		Conv1D_3	256, 20	240
		Conv1D_4	256, 20	240
		Pooling_1	64, 20	0
		Pooling_2	64, 20	0
		Pooling_3	64, 20	0
		Pooling_4	64, 20	0
		Concatenate	64, 80	0
	Stage 2	Conv1D_5	64, 20	17620
		Pooling_5	16, 32	0
Prediction module	LSTM_1		64	6784
	LSTM_2		64	24832
	Dense_1		256	16640
Classification module	Flatten_1		320	0
	Dense_2		3	963

4. Numerical results and discussion

Following training, plotting the accuracies and losses of the different models, and determining the test accuracy, the outcomes were compared to those of other research examining the use of BRNN for lung disease detection

analysis. Among the performance indicators considered, recall, F1 score, accuracy, and precision are all included in this recommended task.

(i) The accuracy is measured by taking the ratio of correctly classified data instances to total data instances.The acronyms for each are as follows: FN stands for false negative, FP for false positive, TN for true negative, and TP for true positive.

$$Accuracy = \frac{TP + TN}{TP + TN + FP + FN} \quad (1)$$

(ii). A 1 (high) precision is ideal for a competent classifier. TP increases to 1 when it equals FP plus TP, suggesting that FP is also zero. What the denominator is worth increases compared to the numerator when the accuracy value decreases and the FP increases.

$$Precision = \frac{TP}{TP + FP} \quad (2)$$

(iii) Common names for recall include sensitivity and true positive rate. Here is how it is defined.

$$Recall = \frac{TP}{TP + FN} \quad (3)$$

(iv) The F1-score, a metric that accounts for recall and precision, is explained as follows:

$$F1 - score = 2 * \frac{precision * recall}{precision + recall} \quad (4)$$

Instead of focusing on accuracy, classifiers' sensitivity (actual positive rate) and specificity (valid negative rate) are commonly used in medical diagnostics to assess their effectiveness. The F1-score is calculated to evaluate the overall classification. 2,000 of the 5,856 chest X-ray pictures in the dataset were utilized for training; the remaining 1,000 images depicted regular chest X-rays, and the remaining 1,000 pictures showed chest X-rays with pneumonia. Fifty epochs were used to train the model. Fig 3 demonstrates how the model's accuracy with other related metrics. With 10 epochs, the accuracy progressively rises from 75% to 90%. After training, the model forecasted test picture labels that were not taught to the model during training. In the test image collection, 3,273 images showed chest X-rays with pneumonia, while 583 images showed regular chest X-rays. Our model's accuracy compared to previous research on tuberculosis and COVID-19 shows that it performs better than prior research. The model correctly predicted the labels for 533 pictures out of 583 normal CXR pictures and 3,070 pictures out of 3,273 CXR pictures that showed pneumonia.

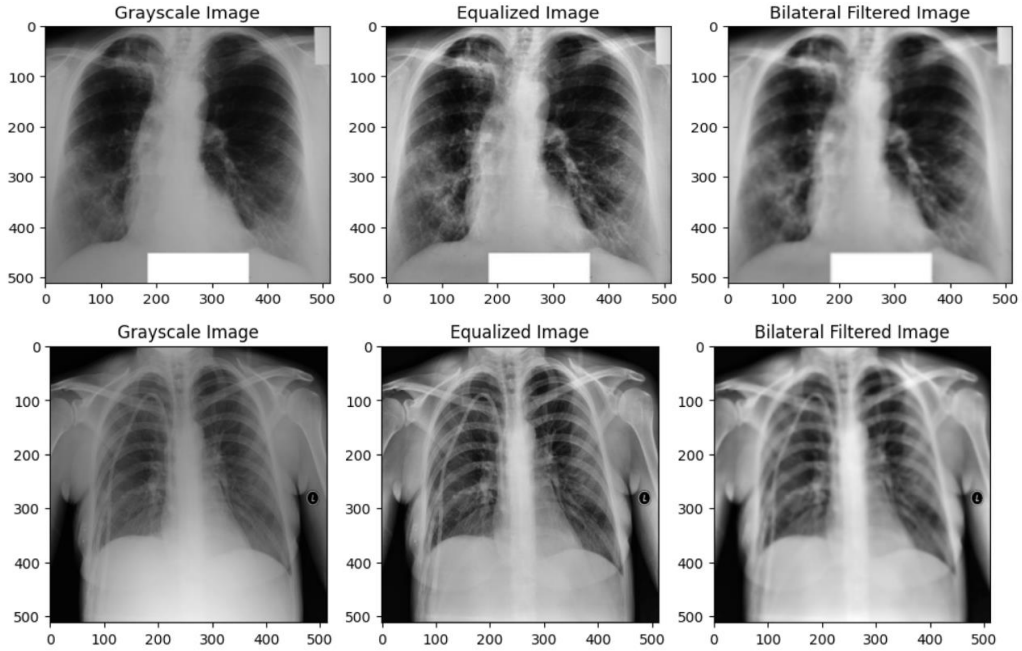

Fig 2a Tuberculosis dataset-based prediction outcomes

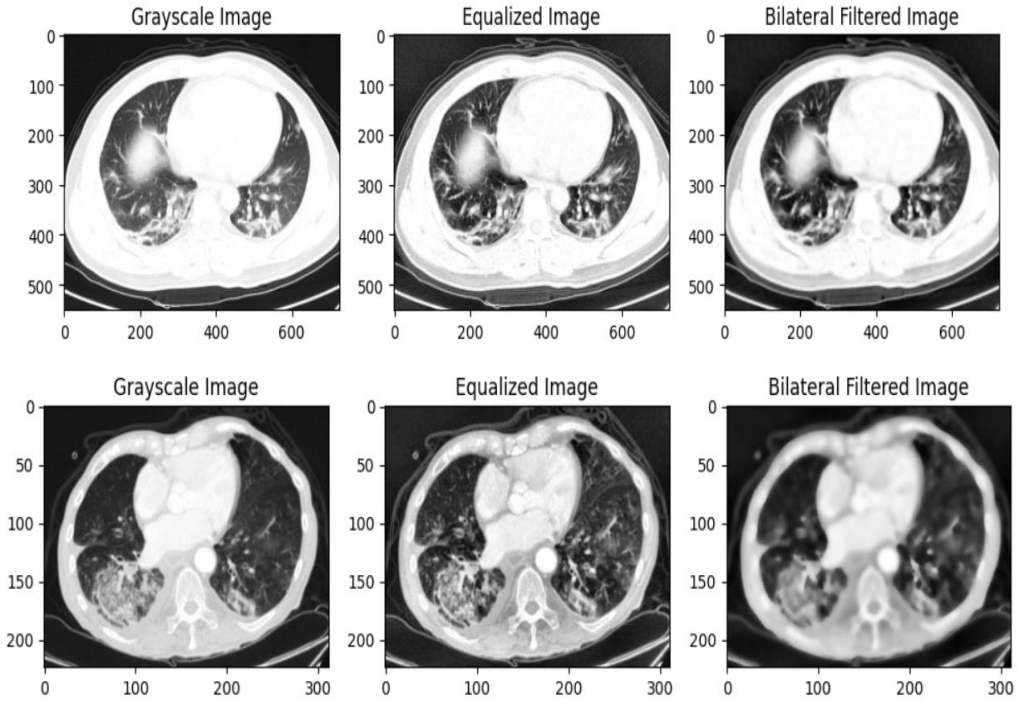

Fig 2b COVID-19 dataset-based filtered image

Six hundred and sixty-six chest X-ray images make up the TB dataset. Of the 662 pictures, 285 displayed a typical chest X-ray, and 292 had a chest X-ray with tuberculosis. These pictures served as instructional material. The tuberculosis model began with a relatively poor accuracy of 50%. Researchers from all across the world have already completed a great deal of studies that have produced encouraging findings. These studies can support currently used techniques or create new avenues for research and development that were previously unattainable. These developments can aid in the quicker and more precise identification and classification of illnesses and offer assistance in achieving remarkable outcomes in eradicating fatal infectious diseases. The test image labels were predicted using the model. There were 85 photos in the test image collection; 41 were of ordinary people, and 44 showed those who had tuberculosis. As shown in Fig 4,the software accurately predicted 39 pictures of individuals with tuberculosis and 37 pictures of ordinary people. The model was trained using 692 photos of individuals with lung disease and 215 images of individuals without lung disease among the total 907 lung CT-scan images in the dataset. The model underwent 100 epochs of training. The model began with an accuracy of 70% and climbed to 90% in roughly 10 epochs. The test images were predicted using the model that was presented. There were 278 photos in the test dataset overall, 224 of which had pneumonia, and 54 were normal. Fig 5 illustrates the loss. The model accurately predicted 54 normal photos and 204 images with pneumonia. Our model's accuracy with previous lung-related research is compared, and we find it to be exceptionally accurate.

clasification report:			precision	recall	f1-score	support
	0		0.00	0.00	0.00	96
	1		0.29	0.22	0.25	76
	2		0.74	1.00	0.85	721
	3		0.00	0.00	0.00	145
accuracy					0.71	1038
macro avg			0.26	0.31	0.28	1038
weighted avg			0.53	0.71	0.61	1038

Fig 3 Evaluation metrics based prediction outcomes

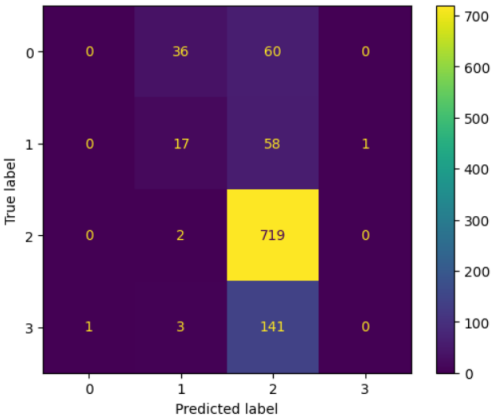

Fig 4 Confusion matrix

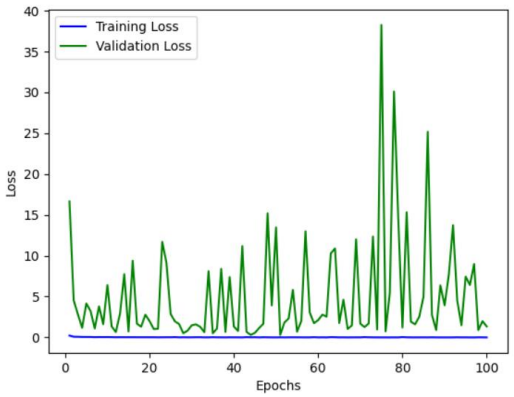

Fig 5 Validation and training loss

The model's accuracy begins at about 81% and rises quickly to 90% in less than five epochs. Fig 3 illustrates how the model's model accuracy for tuberculosis disease gradually improved. For this model, the same dataset where 5,856 photos were utilized, there were a thousand normal chest X-rays and a thousand polluted ones. The model's initial accuracy is perfect because it has previously been trained. The execution process shows slight progress following fifteen epochs of training. There is no continuous development in the accuracy in successive epochsbecause the initial model loss is lower in training and validation. Because the pre-trained models have already been trained on various datasets, Fig 5 demonstrates how simple it is to train them and how the loss progressively drops.

5. Conclusion

Using a variety of lung disorders from the open-source dataset, researchers have presented distinct BRNN architectural model for training. The trained models predicted the labels for a few test photos that the models could not visualize. The suggested models' outcomes fared better than the state-of-the art methods. Regarding F1 score, accuracy, and recall for pneumonia and tuberculosis, the outcomes of utilizing this sequential model with this framework perform better. Moreover, the proposed model performed better in precision and specificity and used less time and computing resources. Tweaking the optimizers and learning rate and adding more data augmentation could improve the classification accuracy of the proposed BRNN models further in the future. To prevent over-fitting, early stopping approaches are expected to offer additional insights into pulmonary disease diagnosis.

REFERENCES

[1] Chandrasekar KS (2022) Exploring the deep-learning techniques in detecting the presence of coronavirus in the chest X-ray images: a comprehensive review. Arch Comput Methods Eng 29:5381–5395
[2] Kieu STH, Bade A, Hijazi MHA, Kolivand H (2020) A survey of deep learning for lung disease detection on medical images: state-of-the-art, taxonomy, issues and future directions. J Imaging 6:131
[3] M. Jasmine Pemeena Priyadarsini, G. Rajini, K. Hariharan, K. Utkarsh Raj, K. Bhargav Ram, V. Indragandhi, V. Subramaniyaswamy, S. Pandya, et al (2023) Lung diseases detection using various deep learning algorithms. J Healthcare Eng 2023:3563696
[4] Amin, S.U.; Alsulaiman, M.; Muhammad, G.; Mekhtiche, M.A.; Hossain, M.S. Deep Learning for EEG motor imagery classification based on multi-layer CNNs feature fusion. Future Gener. Comput. Syst. 2019, 101, 542–554.
[5] Jiang, H.; Ma, H.; Qian, W.; Gao, M.; Li, Y. An Automatic Detection System of Lung Nodule Based on Multi-Group Patch-Based Deep Learning Network. IEEE J. Biomed. Health Inform. 2018, 22, 1227–1237.
[6] Skourt, B.A.; El Hassani, A. Lung CT image segmentation using deep neural networks. Procedia Comput. Sci. 2018, 127, 109–113
[7] Begum, S.; Sarkar, R.; Chakraborty, D.; Maulik, U. Identification of biomarker on biological and gene expression data using fuzzy preference based rough set. J. Intell. Syst. 2021, 30, 130–141.
[8] Razzak, MI; Naz, S.; Zaib, A. Deep learning for medical image processing: Overview, challenges and the future. Lect. Notes Comput. Vis. Biomech. 2018, 26, 323–350.
[9] Roy, R.; Chakraborty, T.; Chowdhury, A.S. A deep learning shape driven level set synergism for pulmonary nodule segmentation. Pattern Recognit. Lett. 2019, 123, 31–38.
[10] Swierczynski, P.; Papie, B.W.; Schnabel, J.A.; Macdonald, C. A level-set approach to joint image segmentation and registration with application to CT lung imaging. Comput. Med. Imaging Graph. 2018, 65, 58–68.

[11] Zhang, W.; Wang, X.; Zhang, P.; Chen, J. Global optimal hybrid geometric active contour for automated lung segmentation on CT images. Comput. Biol. Med. 2017, 91, 168–180.
[12] Ahmed ST, Kadhem SM (2021) Using machine learning via deep learning algorithms to diagnose the lung disease based on chest imaging: a survey. Int J Interact Mob Technol 15:95
[13] Sun J, Liao X, Yan Y, Zhang X, Sun J, Tan W, Liu B, Wu J, Guo Q, Gao S et al (2022) Detection and staging of chronic obstructive pulmonary disease using a computed tomography-based weakly supervised deep learning approach. EurRadiol 32:5319–5329
[14] Bharati S, Podder P, Mondal MRH (2020) Hybrid deep learning for detecting lung diseases from X-ray images. Inf Med Unlocked 20:100391
[15] Wang, J.; Wang, J.; Wen, Y.; Lu, H.; Niu, T.; Pan, J.; Qian, D. Pulmonary Nodule Detection in Volumetric Chest CT Scans Using CNNs-Based Nodule-Size-Adaptive Detection and Classification. IEEE Access 2019, 7, 46033–46044.
[16] Saygili A (2021) Analysis and segmentation of X-ray images of Covid-19 patients using the k-means algorithm. Veri Bilimi 4:1–6
[17] Liu, Y.; Hao, P.; Zhang, P.; Xu, X.; Wu, J.; Chen, W. Dense Convolutional Binary-Tree Networks for Lung Nodule Classification. IEEE Access 2018, 6, 49080–49088
[18] Wang, C.; Chen, D.; Hao, L.; Liu, X.; Zeng, Y.; Chen, J.; Zhang, G. Pulmonary Image Classification Based on Inception-v3 Transfer Learning Model. IEEE Access 2019, 7, 146533–146541
[19] Wang, C.; Shao, J.; Lv, J.; Cao, Y.; Zhu, C.; Li, J.; Shen, W.; Shi, L.; Liu, D.; Li, W. Deep learning for predicting subtype classification and survival of lung adenocarcinoma on computed tomography. Transl. Oncol. 2021, 14, 101141.
[20] Wang, S.; Shi, J.; Ye, Z.; Dong, D.; Yu, D.; Zhou, M.; Liu, Y.; Gevaert, O.; Wang, K.; Zhu, Y.; et al. Using deep learning to predict EGFR mutation status in lung adenocarcinoma on computed tomography image. Eur. Respir. J. 2019, 53, 1800986.
[21] Sumarti H, Sabrina Q, Triana D, Septiani F, Rahmani TPD (2023) Identification of Covid-19 based on features texture histogram and gray level co-occurrence matrix (glcm) using k-means clustering methods in chest X-ray digital images. J Penelitian Fisika Apli 13:51–66
[22] Li, R.; Xiao, C.; Huang, Y.; Hassan, H.; Huang, B. Deep learning applications in computed tomography images for pulmonary nodule detection and diagnosis: A review. Diagnostics 2022, 12, 298.
[23] Manickam M, Siva R, Prabakeran S, Geetha K, Indumathi V, Sethukarasi T (2022) Pulmonary disease diagnosis using african vulture optimized weighted support vector machine approach. Int J Imaging SystTechnol 32:843–856.
[24] Lee, S.M.; Seo, J.B.; Yun, J.; Cho, Y.H.; Vogel-Claussen, J.; Schiebler, M.L.; Gefter, W.B.; van Beek, E.J.; Goo, J.M.; Lee, K.S.; et al. Deep learning applications in chest radiography and computed tomography. J. Thorac. Imaging 2019, 34, 75–85.
[25] Oliver AS, Anuradha M, Justus JJ, Bellam K, Jayasankar T (2020) An efficient coding network based feature extraction with support vector machine based classification model for CT lung images. J Med Imaging Health Inf 10:2628–2633.
[26] Saikia T, Hansdah M, Singh KK, Bajpai MK (2022) Classification of lung nodules based on transfer learning with k-nearest neighbor (knn). In: 2022 IEEE international conference on imaging systems and techniques (IST), IEEE, pp 1–6.
[27] Ashraf, S.F.; Yin, K.; Meng, C.X.; Wang, Q.; Wang, Q.; Pu, J.; Dhupar, R. Predicting benign, pre-invasive, and invasive lung nodules on computed tomography scans using machine learning. J. Thorac. Cardiovasc. Surg. 2022, 163, 1496–1505.
[28] Khan MU, Farman A, Rehman AU, Israr N, Ali MZH, Gulshan ZA (2021) Automated system design for classification of chronic lung viruses using non-linear dynamic system features and k-nearest neighbour. In: 2021 Mohammad Ali Jinnah University International Conference on Computing (MAJICC), IEEE, pp 1–8.
[29] Koureas M, Kirgou P, Amoutzias G, Hadjichristodoulou C, Gourgoulianis K, Tsakalof A (2020) Target analysis of volatile organic compounds in exhaled breath for lung cancer discrimination from other pulmonary diseases and healthy persons. Metabolites 10:317.
[30] Liu C, Zhao R, Pang M (2020) A fully automatic segmentation algorithm for CT lung images based on random forest. Med Phys 47:518–529.